JACC: BASIC TO TRANSLATIONAL SCIENCE
VOL. 1, NO. 4, 2016
ISSN 2452-302X
http://dx.doi.org/10.1016/j.jacbts.2016.04.002

PRE-CLINICAL RESEARCH

Follistatin-Like 1 Regulates Hypertrophy in Heart Failure With Preserved Ejection Fraction

Komei Tanaka, MD, PhD,[a] María Valero-Muñoz, PhD,[a] Richard M. Wilson, BS,[a] Eric E. Essick, PhD,[a] Conor T. Fowler, BS,[a] Kazuto Nakamura, MD, PhD,[a] Maurice van den Hoff, PhD,[b] Noriyuki Ouchi, MD, PhD,[c] Flora Sam, MD[a,d]

VISUAL ABSTRACT

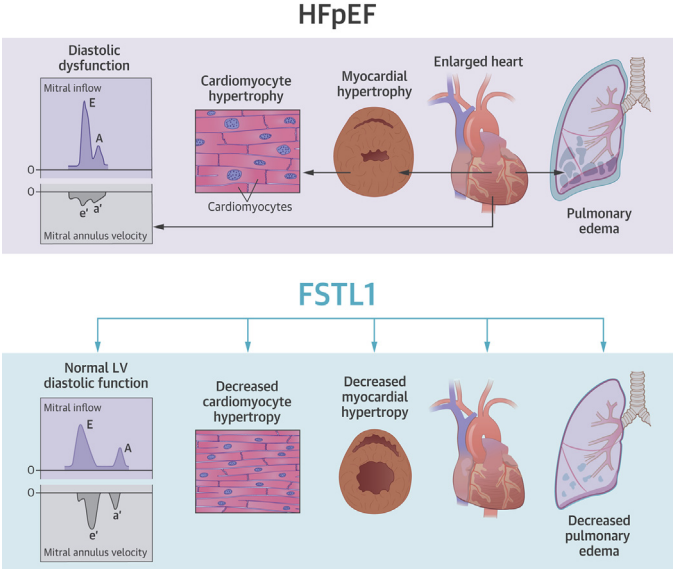

Tanaka, K. et al. J Am Coll Cardiol Basic Trans Science. 2016;1(4):207–21.

HIGHLIGHTS

- **Fstl1, also known as transforming growth factor-β–stimulated clone 36, is an extracellular glycoprotein implicated in the pathophysiology of cardiac disease.**
- **Fstl1 acts in a noncanonical manner relative to other follistatin family members, but its functions remain poorly understood.**
- **Circulating Flst1 levels are increased in humans with chronic stable HFpEF.**
- **Fstl1 treatment modulates cardiomyocyte hypertrophy in vitro and in vivo.**
- **Cardiac myocyte deletion of Fstl1 worsens the HFpEF phenotype in mice.**
- **These studies indicate that Fstl1 may be therapeutically effective in HFpEF by modulating cardiac hypertrophy and improving parameters of diastolic dysfunction.**

From the [a]Whitaker Cardiovascular Institute, Boston University School of Medicine, Boston, Massachusetts; [b]Academic Medical Center, Heart Failure Research Center, Department of Anatomy, Embryology & Physiology, Amsterdam, the Netherlands; [c]Department of Molecular Cardiology, Nagoya University Graduate School of Medicine, Nagoya, Japan; and the [d]Cardiovascular Section and Evans Department of Medicine, Heart Failure Program, Boston University School of Medicine, Boston, Massachusetts.
This work was supported by a grant from the National Institutes of Health (HL117153) to Dr. Sam. All other authors have reported that they have no relationships relevant to the contents of this paper to disclose. Drs. Tanaka and Valero-Muñoz contributed equally to this work.

Manuscript received November 11, 2015; revised manuscript received March 12, 2016, accepted April 6, 2016.

JACC: BASIC TO TRANSLATIONAL SCIENCE VOL. 1, NO. 4, 2016
JUNE 2016:207–21

SUMMARY

Heart failure with preserved ejection fraction (HFpEF) accounts for ~50% of all clinical presentations of heart failure, (HF) and its prevalence is expected to increase. However, there are no evidence-based therapies for HFpEF; thus, HFpEF represents a major unmet need. Although hypertension is the single most important risk factor for HFpEF, with a prevalence of 60% to 89% from clinical trials and human HF registries, blood pressure therapy alone is insufficient to prevent and treat HFpEF. Follistatin-like 1 (Fstl1), a divergent member of the follistatin family of extracellular glycoproteins, has previously been shown to be elevated in HF with reduced ejection fraction and associated with increased left ventricular mass. In this study, blood levels of Fstl1 were increased in humans with HFpEF. This increase was also evident in mice with hypertension-induced HFpEF and adult rat ventricular myocytes stimulated with aldosterone. Treatment with recombinant Fstl1 abrogated aldosterone-induced cardiac myocyte hypertrophy, suggesting a role for Fstl1 in the regulation of hypertrophy in HFpEF. There was also a reduction in the E/A ratio, a measure of diastolic dysfunction. Furthermore, HFpEF induced in a mouse model that specifically ablates Fstl1 in cardiac myocytes (cardiac myocyte-specific Fstl1 knockout [cFstl1-KO]) showed exacerbation of HFpEF with worsened diastolic dysfunction. In addition, cFstl1-KO-HFpEF mice demonstrated more marked cardiac myocyte hypertrophy with increased molecular markers of atrial natriuretic peptide and brain natriuretic peptide expression. These findings indicate that Fstl1 exerts therapeutic effects by modulating cardiac hypertrophy in HFpEF. (J Am Coll Cardiol Basic Trans Science 2016;1:207–21)

Heart failure with preserved ejection fraction (HFpEF) accounts for up to 50% of all heart failure (HF) presentations (1); yet, in contrast to heart failure with reduced ejection fraction (HFrEF), there are no evidence-based therapies. The numerous negative or neutral HFpEF clinical trials, to date, suggest an incomplete mechanistic understanding about HFpEF and the comorbidities that are ubiquitous in HFpEF (2,3). Therefore, the increasing prevalence of this disease and the failure to identify successful therapies for HFpEF suggest that the identification of novel pathways is a priority.

ABBREVIATIONS AND ACRONYMS

ANP = atrial natriuretic peptide
ARVM = adult rat ventricular myocytes
BNP = brain natriuretic peptide
BP = blood pressure
Fstl1 = follistatin-like 1
HFpEF = heart failure with preserved ejection fraction
HFrEF = heart failure with reduced ejection fraction
HR = heart rate
HTN = hypertension
IVST = interventricular septum wall thickness
LV = left ventricular
LVEDD = left ventricular end-diastolic diameter
LVEF = left ventricular ejection fraction
LVH = left ventricular hypertrophy
LVPWT = left ventricular posterior wall thickness

SEE PAGE 222

Despite associated comorbidities, such as obesity and diabetes mellitus, hypertension (HTN) remains *the* most important risk factor for HFpEF, with a prevalence of 60% to 89% reported in large controlled trials, epidemiological studies, and HF registries (1). The presence of left ventricular hypertrophy (LVH) plays a major pathophysiological role in HFpEF, particularly when associated with HTN (4). Myocardial biopsies obtained from a highly selected, younger patient population with HFpEF demonstrated cardiac myocyte hypertrophy, interstitial fibrosis, and evidence of systemic and myocardial inflammation, and oxidative stress (5,6). Therefore, an improved understanding of the HFpEF phenotype, particularly LVH, may provide insights into the development of new therapies for the treatment of HFpEF (7).

Follistatin-like 1 (Fstl1), also known as transforming growth factor-beta–stimulated clone 36, is an extra-cellular glycoprotein that was originally cloned from a mouse osteoblastic cell line as a transforming growth factor-beta–inducible gene and is highly conserved across species (8). Fstl1 acts in a noncanonical manner relative to other follistatin family members. However, its functions remain poorly understood and are possibly cell-type specific. Transduction of Fstl1 into cancer cell lines suppresses growth and invasion (9). Fstl1 is reported to have both anti-inflammatory (10) and proinflammatory (11) actions. Recent studies also implicate Fstl1 in the pathophysiology of cardiac disease in several murine models. Fstl1 overexpression minimized ischemia-reperfusion injury and diminished apoptosis (12). Similarly, Fstl1 improved endothelial cell function and revascularization in a hind-limb ischemia model (13). Recently, we demonstrated elevated blood levels of Fstl1 in a cohort of humans with chronic, stable HFrEF; where elevated Fstl1 levels were significantly associated with LV mass and circulating brain natriuretic peptide (BNP) levels, suggesting a pathogenic role for Fstl1 in cardiac remodeling and LVH (14). In patients with HFpEF, more often than not, structural changes such as LVH are present, because HTN is a major risk factor for the development of LVH (1).

We previously utilized a murine model of HFpEF, which demonstrates features consistent with HFpEF in humans (15–17). HFpEF mice exhibit exercise

intolerance (one of the earliest symptoms of HFpEF in humans), moderate HTN, pulmonary congestion, diastolic dysfunction, and LVH with preserved left ventricular ejection fraction (LVEF). In the present study, we sought to determine whether Fstl1 plays a role in the regulation of cardiac hypertrophy in HFpEF.

METHODS

IN VIVO MURINE MODEL. The Institutional Animal Care and Use Committee at Boston University School of Medicine approved all study procedures related to the handling and surgery of the mice.

Experimental model. Cardiac myocyte-specific Fstl1 knockout (cFstl1-KO) mice in an FVB background were generated as previously described (18). Briefly, mice with loxP sites flanking the exon 1 of the Fstl1 gene (Fstl1flox/flox) were crossed with mice overexpressing Cre recombinase under the control of the α-myosin heavy chain promoter (The Jackson Laboratory, Bar Harbor, Maine). 10- to 12-week-old male/female cFstl1-KO mice and their wild-type (WT) littermates were anesthetized with 80 to 100 mg/kg ketamine and 5 to 10 mg/kg xylazine intraperitoneally. All mice underwent uninephrectomy and received either a continuous infusion of saline (Sham) or *d*-aldosterone (0.15 μg/h, Sigma-Aldrich Co., St. Louis, Missouri) (HFpEF) for 4 weeks via osmotic minipumps (Alzet, Durect Corp., Cupertino, California) (16). All mice were maintained on standard rodent chow and 1.0% sodium chloride drinking water. The 4 groups studied were: WT mice infused with saline (WT-Sham); cFstl1-KO mice infused with saline (cFstl1-KO-Sham); WT mice infused with *d*-aldosterone (WT-HFpEF); and cFstl1-KO mice infused with *d*-aldosterone (cFstl1-KO-HFpEF). Mice were randomly assigned to each experimental group.

Physiological measurements. Heart rate (HR) and blood pressure (BP) were measured weekly using a noninvasive tail-cuff blood pressure analyzer (BP-2000 Blood Pressure Analysis System, Visitech Systems, Inc., Apex, North Carolina). After 4 weeks of saline or *d*-aldosterone infusion, transthoracic echocardiography was performed using the Vevo 770 High-Resolution In Vivo Micro-Imaging System and a Real-Time Micro Visualization 707B Scanhead (VisualSonic Inc., Toronto, Ontario, Canada), as previously described (16). Briefly, to assess diastolic function, mice were anesthetized with isoflurane (0.5% for induction followed by 0.5% to 1.5% for maintenance) and maintained at an HR of ~350 beats/min, because diastolic function is sensitive to HR and loading conditions. The maximum dose of isoflurane had minimal effects on diastolic function (16,19). Pulse wave measurements were recorded. Interventricular septum wall thickness (IVST), LV posterior wall thickness (LVPWT), LV end-diastolic diameter (LVEDD), LV end-systolic diameter, and LVEF were obtained. Total wall thickness was derived from an average of the IVST and LVPWT. LV mass was calculated using the formula: LV mass $= 1.05 \times [(\text{LVEDD} + \text{IVST} + \text{PWT})^3 - (\text{LVEDD})^3]$, as described by Kiatchoosakun et al. (20). After these measurements, mice were sacrificed, and the ratio of wet to dry lung weight was used as an indicator of pulmonary congestion.

Adenoviral vector experiments. Another group of WT mice underwent the same surgical procedures as outlined in the previous text. Fourteen days after surgery, mice were injected in the jugular vein with 1×10^9 plaque-forming units of adenoviral constructs encoding Fstl1 (Ad-Fstl1) or expressing β-galactosidase (Ad-βgal): 1) WT-saline plus Ad-βgal; 2) WT-aldosterone plus Ad-βgal; 3) WT-saline plus Ad-Fstl1; and 4) WT-aldosterone plus Ad-Fstl1. After 14 days, analyses were performed and then mice were killed. Prior studies showed that this adenovirus delivery model led to transduction of Fstl1 in the liver but not the heart, thereby allowing the assessment of the cardioprotective properties of the secreted form of Fstl1 (12,21).

Serum aldosterone. After mice were sacrificed, blood was obtained to determine serum aldosterone levels using an enzyme immunoassay (Alpha Diagnostic Intl. Inc., San Antonio, Texas) (16).

Histopathological analysis. Paraffin-embedded sections of the midventricle (5 μm) were stained with hematoxylin and eosin and Masson trichrome staining to assess LV cardiac myocyte cross-sectional area and myocardial fibrosis as previously described (16). These sections were analyzed, blinded to group identity. Fstl1 staining was assessed as previously described (18). Digital images of stained sections were acquired using an Olympus BX41 Clinical Microscope (Olympus America Inc., Center Valley, Pennsylvania) and analyzed using ImageJ (National Institutes of Health, Bethesda, Maryland).

RNA isolation and quantitative real-time PCR. Total RNA was extracted, and cDNA was synthesized as previously described (16). qRT-PCR was performed with SYBR Green PCR Master Mix (Life Technologies Corporation, Carlsbad, California) in a ViiA7 PCR system (Life Technologies Corporation). Primer sequences are shown in **Table 1**.

Western blot analysis. Protein extraction and western blot analysis were performed as described previously (16,22).

TABLE 1 Primer Sequences Used in qRT-PCR

	Forward	Reverse
Mouse ANP	ATCTGCCCTCTTGAAAAGCA	AAGCTGTTGCAGCCTAGTCC
Mouse BNP	GTCCAGCAGAGACCTCAAAA	AGGCAGAGTCAGAAACTGGA
Mouse collagen 1	CAGAAGATGTAGGAGTCGAG	GGACCCAAGGGAGACCCTGG
Mouse collagen 3	GTGGACTGCCTGGACCTCCA	GGTATCAAAGGCCCAGCTGG
Mouse Fstl1	AACAGCCATCAACATCACCACTTAT	TTTCCAGTCAGCGTTCTCATCA
Mouse GAPDH	CCAAGGTCATCCATGACAACT	GGGCCATCCACAGTCTTCT
Rat ANP	GCTGCTTTGGGCAGAAGATA	AGAGTCTGCAGCCAGGAGGT
Rat GAPDH	CTGCACCACCAACTGCTTAG	CTTCTGAGTGGCAGTGATGG

ANP = atrial natriuretic peptide; BNP = brain natriuretic peptide; GAPDH = glyceraldehyde 3-phosphate dehydrogenase.

HUMAN STUDIES. Written informed consent was obtained from all participants prior to the collection of clinical samples. The study was approved by the Boston University Medical Center Institutional Review Board and conducted according to Declaration of Helsinki principles.

Subjects. Control subjects were healthy, without HF or known cardiac disease (n = 8). They had normal BP and were not taking cardiovascular medications. Patients with HFpEF were enrolled from the outpatient HF Clinic at Boston Medical Center (n = 32). Patients with stable HFpEF were included if they were previously admitted with HF to an inpatient HF service within the prior year and had an LVEF >50% as measured by echocardiogram within 6 months prior to enrollment. Echocardiographic evaluation determined structure and chamber dimensions. Patients with infiltrative disease (e.g., amyloid), a genetic cardiomyopathy (e.g., hypertrophic obstructive cardiomyopathy), or a family history of sudden cardiac death and restrictive disease (e.g., constrictive pericarditis) were excluded. HFpEF etiology was defined as: 1) *hypertensive:* documented history of pharmacologically treated HTN; 2) *ischemic:* prior history of myocardial infarction (electrocardiogram/positive troponin), results of a positive noninvasive stress test, or cardiac catheterization; and 3) *unknown:* having no identifiable cause of the cardiomyopathy. New York Heart Association functional classification, a functional assessment of HF symptoms, was determined (1).

Serum samples were obtained in the outpatient clinic from hemodynamically stable patients with HFpEF who had no evidence of acute decompensation or acute renal failure. After informed consent, blood samples were obtained using routine venipuncture procedure. Samples were centrifuged at 2,000 *g* for 15 min within 1 h from collection. Serum samples were then aliquoted and stored at −80°C.

Serum Fstl1. Total circulating levels of Fstl1 were measured in serum samples by enzyme-linked immunoassay according to the manufacturer's instructions (USCN Life Science Inc., Wuhan, Hubei, China). Standard, controls, and samples were measured in triplicate and averaged. The protein concentrations were calculated using a standard curve generated with recombinant standards provided by the manufacturer. We performed a spike and recovery assay to verify that the enzyme-linked immunosorbent assay did not cross-react with related proteins, such as follistatin or follistatin-like 3.

Laboratory values. BNP and cardiac troponin I (TnI) were measured as part of routine laboratory testing.

Echocardiography. Both 2-dimensional and Doppler echocardiography were performed as previously described (14) using the Vingmed Vivid Five System (GE Healthcare) with a 2.5-Mhz phased-array transducer. Echocardiograms were performed and analyzed in a blinded manner. Measurements of systolic and diastolic chamber dimensions and wall thickness were obtained from 2-dimensional imaging according to the recommendations of the American Association of Echocardiography (23,24). The standard cube formula was utilized to calculate LV mass. Relative wall thickness was calculated as: (2 × LVPWT) / LVEDD.

IN VITRO STUDIES. Isolation and treatment of adult rat cardiac myocytes. Primary cultures of adult rat ventricular cardiac myocytes (ARVM) were prepared as described previously (22,25). ARVM were pre-treated with or without 100 ng/ml recombinant human Fstl1 protein (rFstl1) for 30 min and were then treated with *d*-aldosterone (Sigma-Aldrich Co.).

Preparation of recombinant human Fstl1 protein. rFstl1 tagged with FLAG in the N terminus was prepared in Sf9 cells with minor modifications of the procedure as previously described (26).

[^{3}H]-leucine incorporation assay. Protein synthesis as an indication of cardiac myocyte hypertrophy was measured using a [^{3}H]-leucine incorporation assay (22).

STATISTICAL ANALYSIS. Statistical significance of differences between the 2 groups was assessed by 2-tailed unpaired Student *t* tests. One-way ANOVA and the Newman-Keuls post-hoc test were used to test for differences among at least 3 groups. In cases where the data was not normally distributed, a Kruskal-Wallis test followed by a Dunn test was used. A p value ≤0.05 was considered statistically significant. All statistical analyses were performed using GraphPad Prism (GraphPad Software, Inc. La Jolla, California).

FIGURE 1 **Fstl1 Levels Are Increased in HFpEF**

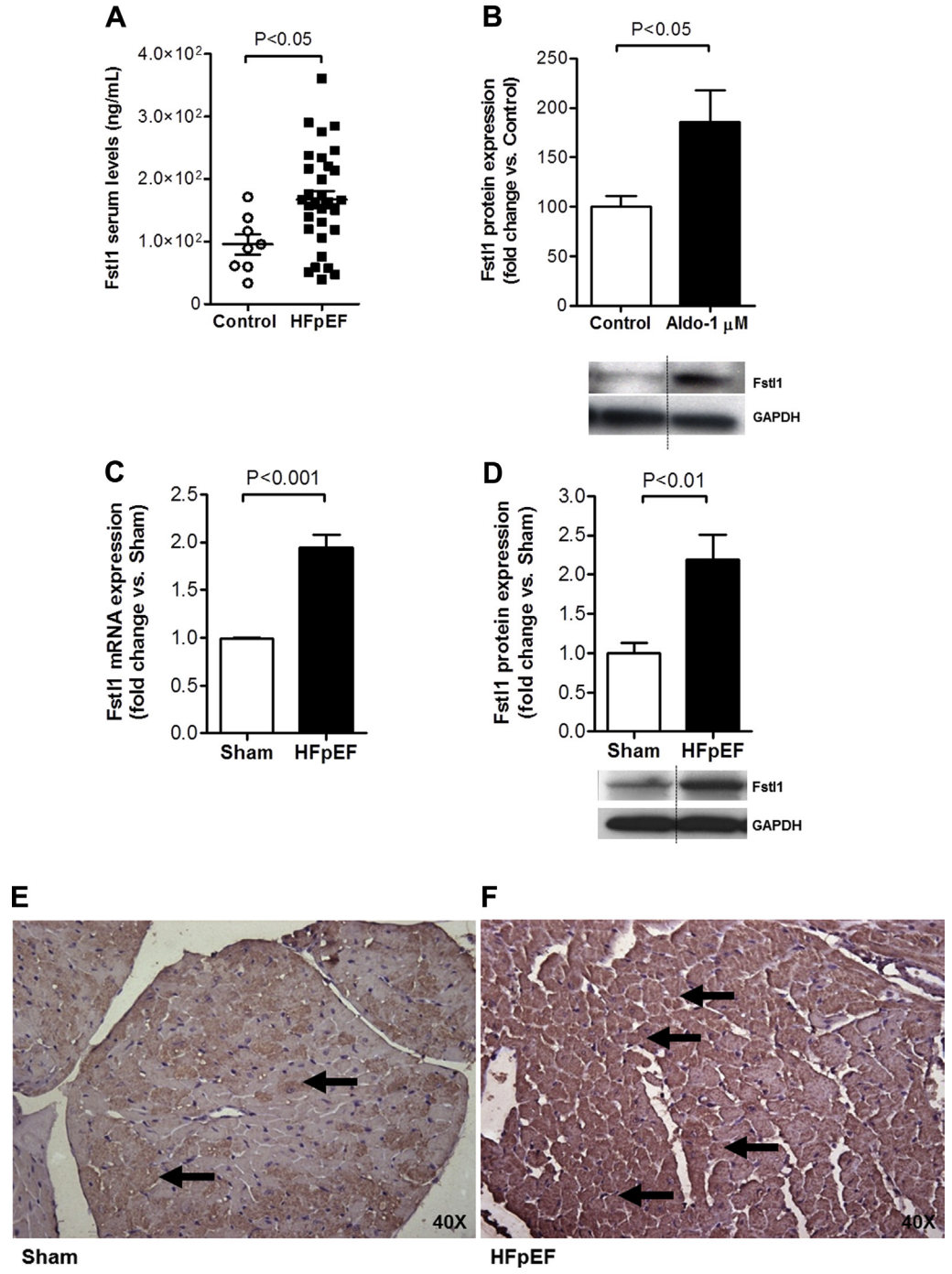

(A) Follistatin-like 1 (Fstl1) serum levels in patients with heart failure with preserved ejection fraction (HFpEF) (n = 32) versus control subjects (Control) (n = 8). **(B)** Fstl1 protein levels in adult rat cardiac myocytes (ARVM) stimulated with aldosterone (Aldo) 1 μmol/l (n = 5 per group). **(C)** Fstl1 mRNA and **(D)** protein levels and representative immunohistochemistry of Fstl1 staining in the left ventricle of Sham **(E)** and HFpEF **(F)** mice (n = 5 to 7 mice/group). **Black arrows in E and F** indicate Fstl1 staining. Data are mean ± SEM. Statistical analysis by 2-tailed Student *t* test. GAPDH = glyceraldehyde 3-phosphate dehydrogenase.

RESULTS

Fstl1 LEVELS ARE INCREASED IN PATIENTS WITH CHRONIC STABLE HFpEF. Similar to our prior findings in HFrEF (14), we observed elevated Fstl1 levels in patients with chronic, stable HFpEF compared with control subjects (167.2 ± 14.0 ng/ml vs. 95.6 ± 16.0 ng/ml; p = 0.018) (Figure 1A). A total of 74% of the patients were black and 55% were women, and patients had associated comorbidities such as HTN (90%), obesity (90%), and diabetes mellitus (58%). LVEF was preserved (63 ± 1%) with mean LV mass of 187.5 ± 9.1 g (normal <162 g). Mean New York Heart Association functional class was 2.1 ± 0.1 at the time of enrollment (Table 2). Diastolic dysfunction was present in 68% of these patients with HFpEF. This cohort of HFpEF patients was similar to those recruited for the I-PRESERVE (Irbesartan in HFpEF trial), in which 69% of patients had evidence of diastolic dysfunction before medication randomization (27).

CARDIAC MYOCYTE STRESS INDUCES Fstl1 EXPRESSION. Cardiac conditions such as HTN or myocardial infarction and neurohormonal activation (e.g., angiotensin II and endothelin) may induce cardiac myocyte hypertrophy (28). Although initially compensatory, if the stressor remains unchecked it may result in decompensated cardiac hypertrophy, with LV dilation, contractile dysfunction, and subsequent clinical HF (29). Because aldosterone stimulation of ARVM induces a stress phenotype (30,31), we investigated whether cardiac myocytes treated with aldosterone induced changes in Fstl1 expression in vitro. ARVM stimulated with a pathophysiological dose (30) of aldosterone (1 μmol/l for 18 h) increased Fstl1 expression (p = 0.032) (Figure 1B).

Next, we sought to establish if the findings seen in humans with HFpEF and ARVM could be recapitulated in a murine model of HFpEF (15,16,32). As previously reported, chronic aldosterone infusion caused HFpEF in mice, with moderate HTN, LVH, pulmonary congestion, and echocardiographic evidence of diastolic dysfunction, while maintaining a preserved LVEF (15,16,32). Fstl1 mRNA and protein expression in the LV of mice with HFpEF were increased 2-fold (p = 0.001 and p = 0.005 vs. Sham mice, respectively) (Figures 1C and 1D). This was confirmed with immunostaining, which showed marked staining of Fstl1 in the LV of HFpEF compared with Sham mice (Figures 1E and 1F). These results thus showed that Fstl1 expression is expressed and up-regulated during cardiac myocyte stress and HFpEF.

TABLE 2 Characteristics of Ambulatory, Stable Patients With HFpEF

	Values	Normal Values
Clinical characteristics		
Age, yrs	65 ± 2	
Male/female	45/55	
Race		
White	23	
Black	74	
Other (Asian, unknown, Hispanic)	3	
Etiology of HFpEF		
Ischemic	3	
Hypertensive/ nonischemic/unknown	97	
Comorbidities		
Obesity: body mass index >30 kg/m^2	90	
Hypertension	90	
Type 2 diabetes mellitus	58	
Systolic blood pressure, mm Hg	129 ± 26	
Diastolic blood pressure, mm Hg	75 ± 10	
Heart rate, beats/min	79 ± 2	
QRS duration, ms	103 ± 24	
NYHA functional class	2.1 ± 0.1	
Echocardiography		
LVEF, %	63 ± 1	
IVS, mm	11.5 ± 0.5	7–11
PW, mm	11.3 ± 0.4	6–11
LVEDD, mm	45.5 ± 1.1	<57
LVESD, mm	31 ± 13	21–40
RWT	0.50 ± 003	0.22–0.42
LV mass, g	187.5 ± 9	67–162
LAVI, ml/m^2	38.1 ± 5	16–34
Diastolic function		
Normal	32	
Grade I diastolic dysfunction	42	
Grade 2 diastolic dysfunction	23	
Grade 3 diastolic dysfunction	3	
Laboratory values		
Cardiac TnI, mg/ml	0.025 ± 0.005	<0.033
BNP, pg/ml	242 ± 47	<100
Creatinine, mg/dl	1.44 ± 0.13	0.7–1.3
MDRD eGFR, ml/min/1.73 m^2	51.6 ± 2.6	>60
Sodium, mmol/l	139 ± 0.8	135–145
Glucose, mg/dl	136 ± 15	70–100

Values are mean ± SD for continuous variables or numbers or percent (%) for categorical variables. Normal values represent normals from 2D echocardiographic parameters and standard normal values for routine laboratory. Grade I diastolic dysfunction: impaired relaxation; grade 2 diastolic dysfunction: pseudonormal filling pattern; and grade 3 diastolic dysfunction: reversible restrictive filling pattern.

BNP = brain natriuretic peptide; IVS = intraventricular septal thickness; LAVI = left atrial volume index; LV = left ventricular; LVEDD = left ventricular end-diastolic diameter; LVEF = left ventricular ejection fraction; LVESD = left ventricular end-systolic diameter; MDRD eGFR = glomerular filtration rate by Modification of Diet in Renal Disease equation; NYHA = New York Heart Association; PW = posterior wall thickness; RWT = relative wall thickness; TnI = troponin I.

Fstl1 MODULATES CARDIAC HYPERTROPHY IN VITRO AND IN VIVO. Given the increased LV expression of Fstl1 in mice with HFpEF, we next examined whether Fstl1 had a direct effect on cardiac myocyte hypertrophy. ARVM were pre-treated with recombinant Fstl1 protein (rFstl1, 100 ng/ml for 30 min) and then stimulated with aldosterone (1 μmol/l for 18 h). At the cellular level, cardiac myocyte hypertrophy is characterized by an increase in cell size and enhanced protein synthesis (7). Thus, to assess cardiac myocyte hypertrophy, protein synthesis was measured by [^{3}H]-Leucine incorporation assay. As showed in Figure 2A, aldo significantly increased [^{3}H]-Leucine incorporation by 2.6-fold compared with control ($p < 0.001$). This increase was completely abrogated by rFstl1 pre-treatment ($p < 0.001$ vs. aldosterone alone). In ARVM, aldosterone also increased ANP gene expression, a molecular marker of cardiac myocyte hypertrophy (33) ($p < 0.01$ vs. control) (Figure 2B), and similarly, pre-treatment with rFstl1 decreased ANP expression by 34% in response to aldosterone ($p < 0.001$). These results are similar to prior findings in neonatal rat ventricular myocyte showing that Fstl1 attenuates the increase in cell surface area induced by phenylephrine (18).

We next investigated if the observed in vitro effects were reproducible in vivo. To examine whether adenovirus-Fstl1 (Ad-Fstl1) supplementation decreased cardiac hypertrophy in HFpEF mice, both WT-aldosterone (HFpEF) and WT-saline (Sham) mice were treated with either Ad-Fstl1 (1×10^9 plaque-forming units) or Ad-β-galactosidase (Ad-βgal), which was injected intravenously 14 days after surgery. Neither Ad-Fstl1 nor Ad-βgal had an effect on systolic BP in Sham or HFpEF mice (data not shown). Treatment with Ad-Fstl1 significantly reduced cardiac hypertrophy in HFpEF, as assessed by the heart weight to body weight ratio, when compared with Ad-βgal (4.75 ± 0.04 mg/g vs. 5.27 ± 0.17 mg/g; $p < 0.01$). Ad-Fstl1 had no effect on heart weight in saline-infused mice (4.17 ± 0.04 mg/g vs. Ad-βgal: 3.90 ± 0.05 mg/g; p = NS) (Figure 3A). Treatment with Ad-Fstl1 also ameliorated a measure of diastolic dysfunction. The E/A ratio was significantly reduced with Ad-Fstl1 (1.88 ± 0.10 vs. Ad-βgal: 1.50 ± 0.10; $p < 0.05$) (Figure 3B). Taken together, these data indicate that treatment with Fstl1 reduces aldosterone-induced cardiac hypertrophy both in vitro and in vivo. In concert with the decreased LVH, the reduced E/A ratio also suggests an improvement in diastolic dysfunction.

CARDIAC MYOCYTE DELETION OF Fstl1 AGGRAVATES THE HFpEF PHENOTYPE IN MICE. To corroborate the hypothesis that Fstl1 is an important modulator of cardiac myocyte hypertrophy in HFpEF, we proceeded to address this in cardiac myocyte-specific Fstl1-KO mice (cFstl1-KO) (18). There was no detectable baseline phenotype in cFstl1-KO mice. Both cFstl1-KO and WT littermates underwent induction of HFpEF, and mice were sacrificed at the end of 4 weeks. Mice characteristics are summarized in Table 3.

Body weight was comparable between all experimental groups. Systolic BP was measured weekly

FIGURE 2 Treatment With Fstl1 Decreases Cardiac Myocyte Hypertrophy Induced By Aldosterone in Adult Rat Ventricular Myocytes

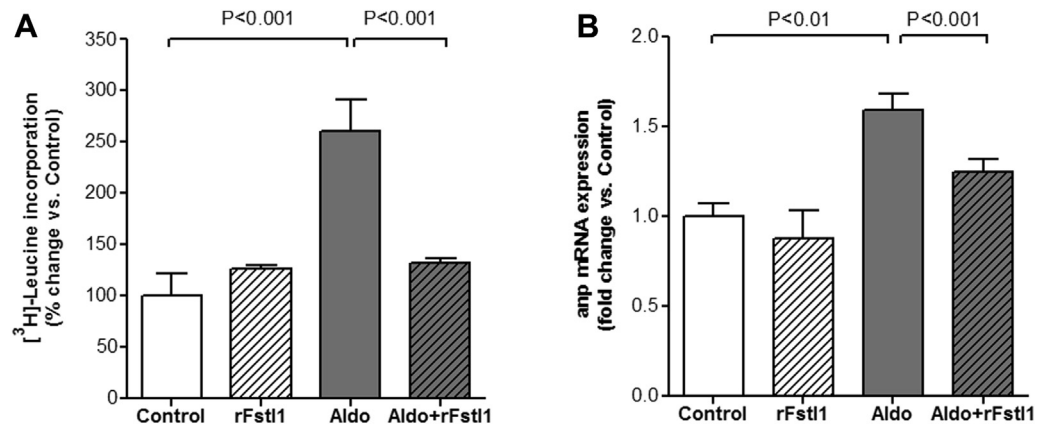

(A) ^{3}H-Leucine incorporation and **(B)** atrial natriuretic peptide (ANP) mRNA expression in adult rat ventricular myocytes after 30-min pre-treatment with 100 ng/ml recombinant human Fstl1 protein (rFstl1) and 18-h treatment with 1 μmol/l aldosterone (Aldo). n = 6 to 12 samples/group. Data are mean ± SEM. Statistical analysis by Kruskal-Wallis test followed by Dunn test. Abbreviations as in Figure 1.

FIGURE 3 Systemic Intravenous Delivery of Fstl1 Ameliorates Cardiac Hypertrophy and Reduces E/A Ratio in Wild-Type HFpEF Mice

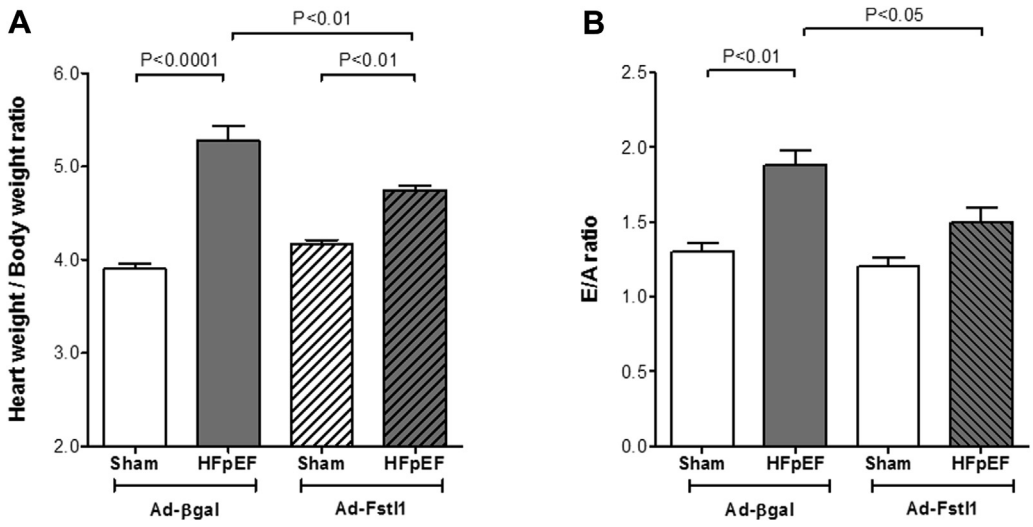

(A) Heart weight/body weight ratio. **(B)** Ratio of peak E velocity to peak A velocity (E/A). Wild-type HFpEF (aldosterone infusion) and Sham (saline infusion) mice were injected, 2 weeks after HFpEF induction, with an adenoviral vector producing either β-galactosidase (Ad-βgal: 1×10^9 plaque-forming units) as control, or Fstl1 (Ad-Fstl1: 1×10^9 plaque-forming units) (n = 3 to 4 mice/group). Data are mean ± SEM. Statistical analysis by analysis of variance (ANOVA) followed by Newman-Keuls multiple comparison tests. Abbreviations as in Figure 1.

(Figure 4A) and was significantly increased after 4 weeks of chronic aldosterone infusion in both WT-HFpEF and cFstl1-KO-HFpEF mice compared with their respective Shams ($p < 0.01$). There was no difference in systolic BP in mice with WT-HFpEF and cFstl1-KO-HFpEF (Table 3).

As expected, chronic aldosterone infusion caused HFpEF and resulted in cardiac hypertrophy, as

TABLE 3 Characteristics of WT and cFstl1-KO Mice With HFpEF—4 Weeks After Chronic Aldosterone (HFpEF) and Saline (Sham) Infusion

	WT-Sham (n = 10)	WT-HFpEF (n = 12)	cFstl1-KO-Sham (n = 10)	cFstl1-KO-HFpEF (n = 12)
Body weight, g	24.3 ± 1.1	25.2 ± 1.0	25.0 ± 1.7	26.5 ± 1.8
Serum aldosterone levels, pg/ml	548 ± 65	6,326 ± 401*	575 ± 71	5,990 ± 325*
Systolic blood pressure, mm Hg	120 ± 2	139 ± 4†	116 ± 4	138 ± 5†
Heart rate, beats/min	691 ± 21	702 ± 13	694 ± 17	669 ± 23
LV structure and systolic function				
TWT, mm	0.87 ± 0.01	1.11 ± 0.02†	0.90 ± 0.01	1.27 ± 0.02†‡
LVEDD, mm	3.52 ± 0.06	3.28 ± 0.13	3.43 ± 0.10	3.35 ± 0.13
LVESD, mm	1.75 ± 0.09	1.57 ± 0.07	1.63 ± 0.09	1.58 ± 0.11
LVEF, %	82.03 ± 1.82	84.26 ± 1.06	84.30 ± 1.65	84.78 ± 1.63
LV diastolic function				
Peak E velocity, mm/s	842.28 ± 18.44	1,006.09 ± 21.93†	834.46 ± 36.65	1,163.30 ± 70.20†§
Peak A velocity, mm/s	661.57 ± 16.69	707.41 ± 17.46	634.72 ± 16.61	656.55 ± 24.61
E/A	1.28 ± 0.03	1.43 ± 0.05‖	1.31 ± 0.04	1.77 ± 0.07†‡
DT, ms	21.43 ± 0.57	20.78 ± 0.58	21.00 ± 0.61	18.13 ± 0.36†§
IVRT, ms	21.07 ± 0.64	19.53 ± 0.33‖	20.45 ± 0.74	13.75 ± 0.51†‡
Peak e′ velocity, mm/s	25.56 ± 0.98	19.27 ± 0.28†	25.58 ± 1.13	16.57 ± 0.50†‡
E/e′	33.16 ± 1.04	52.29 ± 1.34†	32.68 ± 1.03	70.09 ± 2.77†‡

Values are mean ± SEM. Body weight, hemodynamic parameters, blood chemical analysis, LV structure, and systolic and diastolic function in mice. Statistical analysis by analysis of variance followed by Newman-Keuls multiple comparison tests. *$p < 0.001$ vs. respective Sham. †$p < 0.01$ vs. respective Sham. ‡$p < 0.01$ vs. WT-HFpEF. §$p < 0.05$ vs. WT-HFpEF. ‖$p < 0.05$ vs. respective Sham.

A = peak late transmitral flow velocity; cFstl1-KO = follistatin-like 1 cardiac myocyte-specific knockout; DT = early filling deceleration time; E = peak early transmitral flow velocity; e′ = peak early diastolic mitral annular velocity; E/A = the ratio of peak E velocity to peak A velocity; IVRT = isovolumetric relaxation time; TWT = total wall thickness; WT = wild-type; other abbreviations as in Table 2.

FIGURE 4 HFpEF Is Aggravated in Cardiac Myocyte-Specific Fstl1 KO Mice

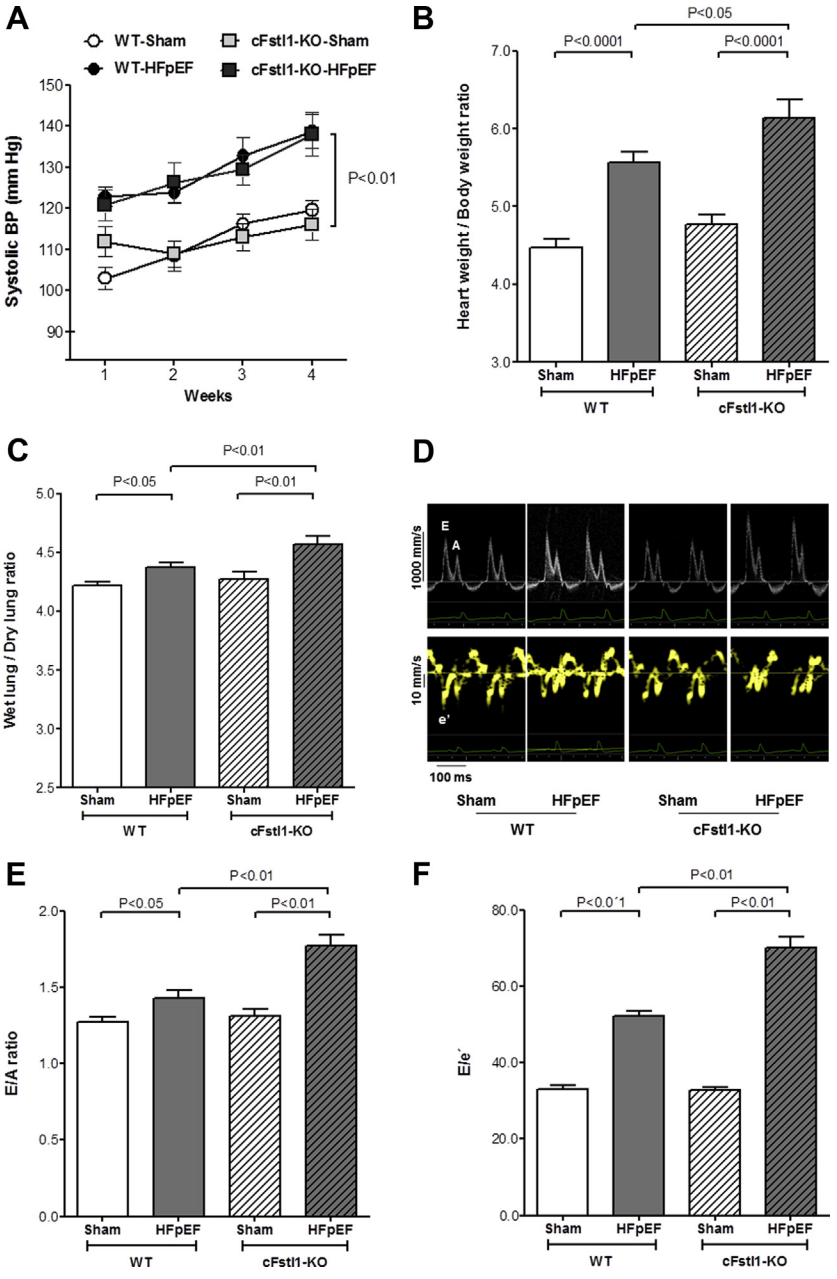

(A) Tail cuff systolic blood pressure (BP) recorded weekly for 4 weeks in wild-type (WT) and cFslt1-KO mice infused with aldosterone (HFpEF) or saline (Sham) (n = 10-12 mice per group). **(B)** Heart weight/body weight ratio and **(C)** wet lung/dry lung ratio in WT and cardiac myocyte-specific Fstl1 knockout (cFslt1-KO) mice (n = 5 to 10 mice/group). Diastolic function assessed 4 weeks after aldosterone (HFpEF) or saline (Sham) infusion in WT and cFslt1-KO mice (n = 10 to 12 mice/group). **(D)** Representative pulse wave and tissue Doppler images. **(E)** Left ventricular compliance measured as ratio of peak E velocity to peak A velocity (E/A), and **(F)** diastolic filling pressure evaluated as ratio of peak E velocity to peak é velocity. Data are mean ± SEM. Statistical analysis by analysis of variance followed by Newman-Keuls multiple comparison tests. A = peak late transmitral flow velocity; E = peak early transmitral flow velocity; é = peak early diastolic myocardial velocity; other abbreviations as in Figure 1.

measured by an increase in the heart weight to body weight ratio, in WT mice versus respective saline-infusion control mice (5.56 ± 0.14 mg/g vs. 4.46 ± 0.11 mg/g; $p < 0.0001$). Cardiac hypertrophy was, however, greater in cFstl1-KO mice with HFpEF (6.14 ± 0.23 mg/g) than in WT-HFpEF mice ($p < 0.05$) (Figure 4B). Consistent with these findings, total wall thickness, determined by echocardiography, was also increased in both groups of aldosterone-infused mice, but increased more in cFstl1-KO-HFpEF than WT-HFpEF. There were no differences in LVEDD and LV end-systolic diameter between the experimental groups of mice (Table 3).

Both WT-HFpEF and cFstl1-KO-HFpEF mice had a normal LVEF but demonstrated pulmonary congestion. However, there was more lung congestion in cFstl1-KO-HFpEF than WT-HFpEF mice, as measured by an increase in the wet-to-dry lung weight ratio (4.57 ± 0.07 vs. 4.37 ± 0.05; $p < 0.01$) (Figure 4C). Mitral Doppler analysis (Table 3, Figure 4D) showed an increased peak E-wave velocity in both groups of HFpEF mice ($p < 0.01$ vs. respective sham groups). The peak E-wave velocity in cFstl1-KO-HFpEF mice was, however, significantly higher than in WT-HFpEF mice ($p < 0.05$). Because the peak A-wave velocity remained comparable in all groups of mice, the resultant E/A ratio was higher in aldosterone-infused mice, with the greatest increase in the cFstl1-KO-HFpEF mice ($p < 0.01$ vs. WT-HFpEF) (Figure 4E). These results suggest worse LV compliance in cFstl1-KO-HFpEF versus WT-HFpEF mice. Moreover, deceleration time was shortened in cFstl1-KO-HFpEF versus WT HFpEF ($p < 0.05$), implying more impaired LV relaxation. Similar to humans, in whom isovolumetric relaxation time (IVRT) initially increases with impaired relaxation but then decreases with progressive worsening of diastolic function, IVRT was significantly shorter both in mice with WT-HFpEF and with cFstl1-KO-HFpEF ($p < 0.05$ vs. respective Shams). Moreover, cFstl1-KO-HFpEF mice also showed diminished IVRT when compared with WT-HFpEF mice ($p < 0.01$). Tissue Doppler was used to measure mitral annular e′ velocity (Table 3). Aldosterone infusion decreased the peak mitral é velocity in mice with WT-HFpEF ($p < 0.01$ vs. WT-Sham) and was further reduced in cFstl1-KO-HFpEF versus WT-HFpEF mice ($p < 0.01$). Thus, the resultant E/e′ ratio, a measure of diastolic filling pressure, was higher in mice with cFstl1-KO-HFpEF when compared with mice with WT-HFpEF ($p < 0.01$) (Figure 4F).

In summary, these findings indicate that lack of Fstl1 expression in cardiac myocytes exacerbates diastolic dysfunction in mice with HFpEF.

HFpEF EXACERBATION IN cFstl1-KO MICE IS ASSOCIATED WITH CARDIAC MYOCYTE HYPERTROPHY. We next investigated whether the increase in cardiac hypertrophy and exacerbation of HFpEF in cFstl1-KO were also associated with cellular changes, as seen in ARVM.

Histological examination of the LV showed that cardiac myocyte hypertrophy, as measured by cardiac myocyte size, was significantly greater in cFstl1-KO-HFpEF than WT-HFpEF and Sham controls (cFstl1-KO-HFpEF: 341.2 ± 8.5 μm^2 vs. WT-HFpEF: 309.4 ± 13.4 μm^2; $p < 0.05$) (Figure 5A). Furthermore, ANP and BNP mRNA expression were increased in both groups of HFpEF mice ($p < 0.0001$ vs. Sham), but the increase was significantly higher in cFstl1-KO-HFpEF versus WT-HFpEF mice ($p < 0.05$) (Figure 5B). These data supported earlier findings in ARVM indicating that Fstl1 plays a role in cardiac myocyte hypertrophy. Thus, although treatment with Fstl1 modulates cardiac growth in response to cell stress, deficiency of Fstl1 in cardiac myocytes induces more hypertrophy in HFpEF mice.

Fstl1 DELETION DOES NOT AFFECT THE CARDIAC FIBROTIC PHENOTYPE. Cardiac hypertrophy and myocardial fibrosis are commonly seen in the hearts of patients with HFpEF (4) and may be related to comorbidities other than HTN (34). An increase in the collagen content in the myocardium results in myocardial fibrosis, which is considered an endpoint in the pathological process of cardiac remodeling, leading to impaired ventricular function. Thus, the presence of diffuse myocardial fibrosis could be a major determinant of altered diastolic filling and systolic pumping function in the LV (35). We next examined whether deletion of Fstl1 in cardiac myocytes affected myocardial fibrosis in HFpEF. Using Masson trichrome staining to quantify collagen deposition we found that, as expected, aldosterone infusion significantly increased the area of myocardial fibrosis in both groups of mice ($p < 0.05$ vs. respective saline), but was not different between cFstl1-KO-HFpEF and WT-HFpEF mice (3.8 ± 0.9% vs. 2.9 ± 0.8%) (Figure 6A). Similarly, collagen 1 and 3 mRNA expression were significantly higher versus Sham ($p < 0.05$) but were comparable between cFstl1-KO-HFpEF and WT-HFpEF mice (Figure 6B).

These results indicate that Fstl1 plays a pivotal role in cardiac hypertrophy during HFpEF independent of changes in fibrosis.

DISCUSSION

The prevalence of HFpEF continues to increase, but prognosis remains poor. Patients with HFpEF have an

FIGURE 5 Lack of Fstl1 Increases Cardiac Myocyte Hypertrophy in HFpEF Mice

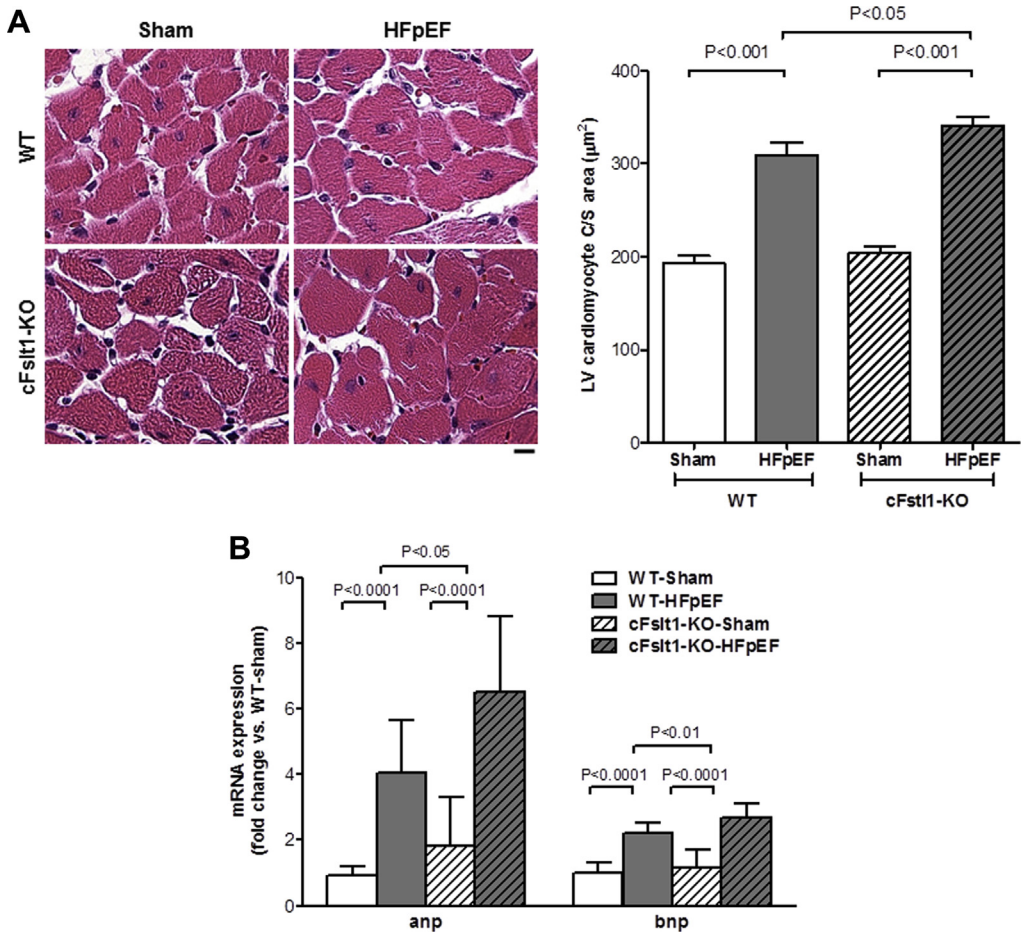

(A) Cardiac myocyte hypertrophy in the left ventricle (LV) **(left,** representative hematoxylin and eosin images, scale bar: 10 μm) and quantitative measure of cardiac myocyte cross-sectional area **(right)**. **(B)** Atrial natriuretic peptide (ANP) and brain natriuretic peptide (BNP) mRNA expression in WT and cFslt1-KO mice with aldosterone (HFpEF) or saline (Sham) infusion. n = 6 to 12 mice/group. Data are mean ± SEM. Statistical analysis by analysis of variance followed by Newman-Keuls multiple comparison tests. Abbreviations as in Figures 1 and 4.

impressive 5-year mortality rate (approaching 60%) and a costly morbidity rate, with approximately 50% of patients being readmitted to the hospital within 6 months (36). Predictors of morbidity and mortality in HFpEF remain incompletely defined (37). In addition, to date, standard HF therapy shown to be effective in HFrEF have no established benefit in HFpEF (38). In fact, recently published HF guidelines concluded that "no treatment has yet been shown, convincingly, to reduce morbidity or mortality in patients with HFpEF" (39).

In search of potential novel therapies for HFpEF, the goal of this study was to investigate the role of Fstl1 in HFpEF. Fstl1 levels were measured in a cohort of stable HFpEF patients and were significantly increased compared with control subjects. Similarly, in vitro and in vivo studies showed increased expression of Fstl1 in cardiac myocytes when ARVM were stimulated with aldo and in a murine model of HFpEF. Deletion of Fstl1 in cardiac myocytes exacerbated cardiac hypertrophy in HFpEF, independent of fibrosis. These changes were accompanied by increased gene expression of natriuretic peptides (ANP and BNP), molecular markers of cardiac myocyte hypertrophy.

In addition to elevated circulating levels of Fstl1 in HF, elevated levels are also seen in acute coronary syndrome (14,40), indicating the importance of this cardiokine in cardiac disease. Murine models of

FIGURE 6 Lack of Cardiac Myocyte Fstl1 in HFpEF Does Not Affect Cardiac Fibrosis

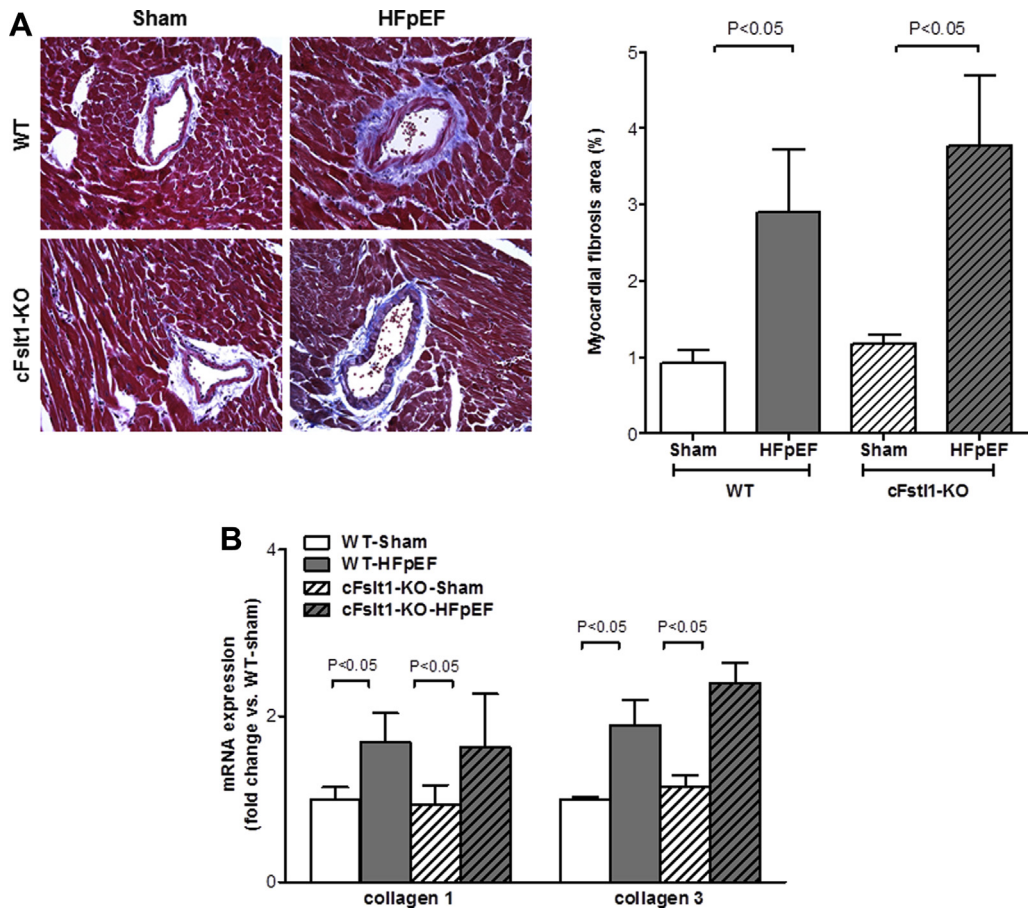

(A) Cardiac fibrosis in the left ventricle (LV) (**left,** representative Masson trichrome images, original magnification ×400) and myocardial fibrosis area **(right)** in WT and cFslt1-KO mice subjected to aldosterone (HFpEF) or saline (Sham) infusion. **(B)** Collagen 1 and 3 mRNA expression in WT and cFslt1-KO mice after aldosterone (HFpEF) or saline (Sham) infusion. n = 6 to 12 mice/group. Data are mean ± SEM. Statistical analysis by analysis of variance followed by **(A)** Newman-Keuls multiple comparison tests and **(B)** Kruskal-Wallis test followed by Dunn test.

cardiac stress, such as myocardial pressure overload or ischemia and reperfusion injury, have also shown increased cardiac expression of Fstl1 (18,41). It has been suggested that cardiac myocytes are a major source of Fstl1 (42) and that cardiac expression of Fstl1 mediates a protective effect via different mechanisms such as antiapoptotic or antihypertrophic actions (18,41). In the present study, therapy with rFslt1 demonstrated an antihypertrophic response in cardiac myocytes stimulated with pathophysiological doses of aldosterone (30). In this chronic aldosterone infusion HFpEF model, circulating levels of aldo are in the range of 6 to 7.5 nmol/l (16,17), which is comparable to levels (~100 nmol/l) seen in acute human HF (43–45). Similar to in vitro findings, treatment with Ad-Fstl1 abrogated cardiac hypertrophy in mice with HFpEF.

Cardiac-specific myocyte deletion of Fstl1 in mice with HFpEF was also associated with marked LVH. This LVH was accompanied by a worsening of diastolic dysfunction as determined by echocardiography. These changes were not associated with changes in systolic BP. In the present study, cardiac myocyte deletion of Fstl1 did not affect BP regulation. Therefore, the observed increase in LVH and worsened diastolic dysfunction were direct consequences of cardiac myocyte deletion of Fstl1-induced changes in the heart.

HFpEF is a disease and clinical syndrome that is associated with different comorbidities and pathophysiologies. The latter includes structural, functional, and metabolic abnormalities (46). LVH is the most common myocardial structural abnormality associated with HFpEF (47). A broad range of molecular pathways are thought to be involved in the development of cardiac hypertrophy, including the release of hormones, cytokines, chemokines, and peptide growth factors (48,49). cFstl1-KO mice with HFpEF displayed a greater increase in cardiac myocyte hypertrophy versus WT-HFpEF mice. In addition, increases in ANP and BNP expression were greatest in HFpEF when there was cardiac myocyte-specific deletion of Fstl1. The molecular mechanisms of Fstl1 in cardiac function and hypertrophy in HFpEF are not fully understood. A major unanswered question is how Fstl1 regulates cardiac myocyte hypertrophy. It has been demonstrated that Akt signaling pathway induces Fstl1 up-regulation in the heart during cardiac injury (12) and that Fstl1 promotes AMPK activation, which may function by suppressing cardiac hypertrophy (18).

Increased cardiac myocyte growth is usually accompanied by an increase in the extracellular matrix, which is predominantly composed of collagen and, to a lesser degree elastin, laminin, and fibronectin (50). The present findings differ from prior reports that suggested Fstl1 plays a role by modulating cardiac (18), renal (42), or pulmonary (51) fibrosis. The observed differences could be due to the experimental model used in the different studies. For example, Shimano et al. (18) utilized a model of pressure overload induced by transverse aortic constriction over 4 weeks in cFstl1-KO, which resulted in *HFrEF with depressed LVEF* and a dilated LV chamber size. These data suggest that there is differential regulation of Fstl1 in cardiac myocyte hypertrophy in HFpEF versus HFrEF.

LVH regression is not always accompanied by improvement in parameters of diastolic dysfunction (52), and conversely, improvement in diastolic dysfunction parameters is not consistently accompanied by LVH regression (15). In the present study, mice with HFpEF, that lack cardiac myocyte-specific Fstl1 showed exacerbation of LVH that was accompanied by worsening of diastolic dysfunction.

Fstl1 displays a Janus-like role in inflammation. Pro-inflammatory actions of Fstl1 are seen in several chronic disorders such as rheumatoid arthritis, ulcerative colitis, and obesity (11,53,54). Conversely the anti-inflammatory role of Fstl1 has also been described in vascular, myocardial, and renal injury models (26,41,42). Moreover, it is unknown whether inflammation plays a key role in HFpEF or is simply a bystander because of various comorbidities (55). Is inflammation up-regulated in a compensatory manner, or is it an epiphenomenon of a catabolic state caused by HF (56)? In this study, the immunomodulatory role of Fstl1 in the pathophysiology of LVH in HFpEF was not addressed.

Therefore, we conclude that Fstl1 exerts therapeutic effects in HFpEF by modulating cardiac hypertrophy. Although there is some knowledge of the pathophysiology and mechanisms of HFpEF, few signaling targets have been identified. The present work represents a “proof-of-concept” study for the role of Fstl1 in HFpEF. We provide cell, animal, and human data to support our hypothesis. The relevance of these translational findings indicates that Fstl1 has an antihypertrophic effect in HFpEF.

REPRINT REQUESTS AND CORRESPONDENCE: Dr. Flora Sam, Whitaker Cardiovascular Institute, Cardiovascular Section, Boston University School of Medicine, 700 Albany Street, W507, Boston, Massachusetts 02118. E-mail: flora.sam@bmc.org.

PERSPECTIVES

COMPETENCY IN MEDICAL KNOWLEDGE: The lack of evidence-based therapies continues to hinder our care and treatment of patients with HFpEF. Therapy has been relegated to symptom control and the management of comorbidities, such as HR and BP control. This is inadequate, and the increasing prevalence of HFpEF highlights the pressing need to identify new mechanistic pathways to target therapy for HFpEF.

TRANSLATIONAL OUTLOOK: HFpEF is a heterogeneous disease with associated comorbidities and risk factors. Limited animal models of HFpEF continue to plague translational studies, and utilizing a murine model may not be entirely complementary to human cardiac disease. However, identifying factors present in patients with HFpEF (such as Fstl1) and exploring the relevance of these factors in a murine model of HFpEF indicate that Fstl1 and its role in cardiac hypertrophy is not a model-specific finding and may contribute to our understanding of the pathogenesis of HFpEF for future drug development. These pre-clinical studies are important not only to test drug therapies, but also to provide insights into signaling pathways important in the pathogenesis of HFpEF.

REFERENCES

1. Yancy CW, Jessup M, Bozkurt B, et al. 2013 ACCF/AHA guideline for the management of heart failure: a report of the American College of Cardiology Foundation/American Heart Association Task Force on practice guidelines. J Am Coll Cardiol 2013;62:e147–239.

2. Mentz RJ, Kelly JP, von Lueder TG, et al. Noncardiac comorbidities in heart failure with reduced versus preserved ejection fraction. J Am Coll Cardiol 2014;64:2281–93.

3. Paulus WJ, Tschope C. A novel paradigm for heart failure with preserved ejection fraction: comorbidities drive myocardial dysfunction and remodeling through coronary microvascular endothelial inflammation. J Am Coll Cardiol 2013;62:263–71.

4. Zile MR, Desantis SM, Baicu CF, et al. Plasma biomarkers that reflect determinants of matrix composition identify the presence of left ventricular hypertrophy and diastolic heart failure. Circ Heart Fail 2011;4:246–56.

5. Westermann D, Lindner D, Kasner M, et al. Cardiac inflammation contributes to changes in the extracellular matrix in patients with heart failure and normal ejection fraction. Circ Heart Fail 2011;4:44–52.

6. van Heerebeek L, Borbely A, Niessen HW, et al. Myocardial structure and function differ in systolic and diastolic heart failure. Circulation 2006;113:1966–73.

7. Frey N, Katus HA, Olson EN, Hill JA. Hypertrophy of the heart: a new therapeutic target? Circulation 2004;109:1580–9.

8. Zwijsen A, Blockx H, Van Arnhem W, et al. Characterization of a rat C6 glioma-secreted follistatin-related protein (FRP). Cloning and sequence of the human homologue. Eur J Biochem 1994;225:937–46.

9. Sumitomo K, Kurisaki A, Yamakawa N, et al. Expression of a TGF-beta1 inducible gene, TSC-36, causes growth inhibition in human lung cancer cell lines. Cancer Lett 2000;155:37–46.

10. Kawabata D, Tanaka M, Fujii T, et al. Ameliorative effects of follistatin-related protein/TSC-36/FSTL1 on joint inflammation in a mouse model of arthritis. Arthritis Rheum 2004;50:660–8.

11. Miyamae T, Marinov AD, Sowders D, et al. Follistatin-like protein-1 is a novel proinflammatory molecule. J Immunol 2006;177:4758–62.

12. Oshima Y, Ouchi N, Sato K, Izumiya Y, Pimentel DR, Walsh K. Follistatin-like 1 is an Akt-regulated cardioprotective factor that is secreted by the heart. Circulation 2008;117:3099–108.

13. Ouchi N, Oshima Y, Ohashi K, et al. Follistatin-like 1, a secreted muscle protein, promotes endothelial cell function and revascularization in ischemic tissue through a nitric-oxide synthase-dependent mechanism. J Biol Chem 2008;283:32802–11.

14. El-Armouche A, Ouchi N, Tanaka K, et al. Follistatin-like 1 in chronic systolic heart failure: a marker of left ventricular remodeling. Circ Heart Fail 2011;4:621–7.

15. Wilson RM, De Silva DS, Sato K, Izumiya Y, Sam F. Effects of fixed-dose isosorbide dinitrate/hydralazine on diastolic function and exercise capacity in hypertension-induced diastolic heart failure. Hypertension 2009;54:583–90.

16. Tanaka K, Wilson RM, Essick EE, et al. Effects of adiponectin on calcium-handling proteins in heart failure with preserved ejection fraction. Circ Heart Fail 2014;7:976–85.

17. Sam F, Duhaney TA, Sato K, et al. Adiponectin deficiency, diastolic dysfunction, and diastolic heart failure. Endocrinology 2010;151:322–31.

18. Shimano M, Ouchi N, Nakamura K, et al. Cardiac myocyte follistatin-like 1 functions to attenuate hypertrophy following pressure overload. Proc Natl Acad Sci U S A 2011;108:E899–906.

19. Zhou YQ, Foster FS, Parkes R, Adamson SL. Developmental changes in left and right ventricular diastolic filling patterns in mice. Am J Physiol Heart Circ Physiol 2003;285:H1563–75.

20. Kiatchoosakun S, Restivo J, Kirkpatrick D, Hoit BD. Assessment of left ventricular mass in mice: comparison between two-dimensional and m-mode echocardiography. Echocardiography 2002;19:199–205.

21. Shibata R, Sato K, Kumada M, et al. Adiponectin accumulates in myocardial tissue that has been damaged by ischemia-reperfusion injury via leakage from the vascular compartment. Cardiovasc Res 2007;74:471–9.

22. Essick EE, Ouchi N, Wilson RM, et al. Adiponectin mediates cardioprotection in oxidative stress-induced cardiac myocyte remodeling. Am J Physiol Heart Circ Physiol 2011;301:H984–93.

23. Devereux RB, Alonso DR, Lutas EM, et al. Echocardiographic assessment of left ventricular hypertrophy: comparison to necropsy findings. Am J Cardiol 1986;57:450–8.

24. Schiller NB, Shah PM, Crawford M, et al. Recommendations for quantitation of the left ventricle by two-dimensional echocardiography. American Society of Echocardiography Committee on Standards, Subcommittee on Quantitation of Two-Dimensional Echocardiograms. J Am Soc Echocardiogr 1989;2:358–67.

25. Essick EE, Wilson RM, Pimentel DR, et al. Adiponectin modulates oxidative stress-induced autophagy in cardiomyocytes. PLoS One 2013;8:e68697.

26. Miyabe M, Ohashi K, Shibata R, et al. Muscle-derived follistatin-like 1 functions to reduce neointimal formation after vascular injury. Cardiovasc Res 2014;103:111–20.

27. Zile MR, Gottdiener JS, Hetzel SJ, et al. Prevalence and significance of alterations in cardiac structure and function in patients with heart failure and a preserved ejection fraction. Circulation 2011;124:2491–501.

28. Yamazaki T, Komuro I, Yazaki Y. Signalling pathways for cardiac hypertrophy. Cell Signal 1998;10:693–8.

29. Drazner MH. The progression of hypertensive heart disease. Circulation 2011;123:327–34.

30. De Silva DS, Wilson RM, Hutchinson C, et al. Fenofibrate inhibits aldosterone-induced apoptosis in adult rat ventricular myocytes via stress-activated kinase-dependent mechanisms. Am J Physiol Heart Circ Physiol 2009;296:H1983–93.

31. Rude MK, Duhaney TA, Kuster GM, et al. Aldosterone stimulates matrix metalloproteinases and reactive oxygen species in adult rat ventricular cardiomyocytes. Hypertension 2005;46:555–61.

32. Garcia AG, Wilson RM, Heo J, et al. Interferon-gamma ablation exacerbates myocardial hypertrophy in diastolic heart failure. Am J Physiol Heart Circ Physiol 2012;303:H587–96.

33. Takemura G, Fujiwara H, Mukoyama M, et al. Expression and distribution of atrial natriuretic peptide in human hypertrophic ventricle of hypertensive hearts and hearts with hypertrophic cardiomyopathy. Circulation 1991;83:181–90.

34. Mohammed SF, Hussain S, Mirzoyev SA, Edwards WD, Maleszewski JJ, Redfield MM. Coronary microvascular rarefaction and myocardial fibrosis in heart failure with preserved ejection fraction. Circulation 2015;131:550–9.

35. Su MY, Lin LY, Tseng YH, et al. CMR-verified diffuse myocardial fibrosis is associated with diastolic dysfunction in HFpEF. JACC Cardiovasc Imaging 2014;7:991–7.

36. Steinberg BA, Zhao X, Heidenreich PA, et al. Trends in patients hospitalized with heart failure and preserved left ventricular ejection fraction: prevalence, therapies, and outcomes. Circulation 2012;126:65–75.

37. Zile MR, Baicu CF. Biomarkers of diastolic dysfunction and myocardial fibrosis: application to heart failure with a preserved ejection fraction. J Cardiovasc Transl Res 2013;6:501–15.

38. Andersen MJ, Borlaug BA. Heart failure with preserved ejection fraction: current understandings and challenges. Curr Cardiol Rep 2014;16:501.

39. McMurray JJ, Adamopoulos S, Anker SD, et al. ESC guidelines for the diagnosis and treatment of acute and chronic heart failure 2012: the Task Force for the Diagnosis and Treatment of Acute and Chronic Heart Failure 2012 of the European Society of Cardiology. Developed in collaboration with the Heart Failure Association (HFA) of the ESC. Eur Heart J 2012;33:1787–847.

40. Widera C, Horn-Wichmann R, Kempf T, et al. Circulating concentrations of follistatin-like 1 in healthy individuals and patients with acute coronary syndrome as assessed by an immunoluminometric sandwich assay. Clin Chem 2009;55:1794–800.

41. Ogura Y, Ouchi N, Ohashi K, et al. Therapeutic impact of follistatin-like 1 on myocardial ischemic injury in preclinical models. Circulation 2012;126:1728–38.

42. Hayakawa S, Ohashi K, Shibata R, et al. Cardiac myocyte-derived follistatin-like 1 prevents renal

injury in a subtotal nephrectomy model. J Am Soc Nephrol 2015;26:636–46.

43. Mano A, Tatsumi T, Shiraishi J, et al. Aldosterone directly induces myocyte apoptosis through calcineurin-dependent pathways. Circulation 2004;110:317–23.

44. Rousseau MF, Gurne O, Duprez D, et al. Beneficial neurohormonal profile of spironolactone in severe congestive heart failure: results from the RALES neurohormonal substudy. J Am Coll Cardiol 2002;40:1596–601.

45. Silvestre JS, Robert V, Heymes C, et al. Myocardial production of aldosterone and corticosterone in the rat. Physiological regulation. J Biol Chem 1998;273:4883–91.

46. Burchfield JS, Xie M, Hill JA. Pathological ventricular remodeling: mechanisms: part 1 of 2. Circulation 2013;128:388–400.

47. Heinzel FR, Hohendanner FR, Jin G, Sedej S, Edelmann F. Myocardial hypertrophy and its role in heart failure with preserved ejection fraction. J Appl Physiol (1985) 2015;jap.

48. Mudd JO, Kass DA. Tackling heart failure in the twenty-first century. Nature 2008;451:919–28.

49. Heineke J, Molkentin JD. Regulation of cardiac hypertrophy by intracellular signalling pathways. Nat Rev Mol Cell Biol 2006;7:589–600.

50. Phan TT, Shivu GN, Abozguia K, Sanderson JE, Frenneaux M. The pathophysiology of heart failure with preserved ejection fraction: from molecular mechanisms to exercise haemodynamics. Int J Cardiol 2012;158:337–43.

51. Dong Y, Geng Y, Li L, et al. Blocking follistatin-like 1 attenuates bleomycin-induced pulmonary fibrosis in mice. J Exp Med 2015;212:235–52.

52. Barron AJ, Hughes AD, Sharp A, et al. Long-term antihypertensive treatment fails to improve E/e′ despite regression of left ventricular mass: an Anglo-Scandinavian cardiac outcomes trial substudy. Hypertension 2014;63:252–8.

53. Fan N, Sun H, Wang Y, et al. Follistatin-like 1: a potential mediator of inflammation in obesity. Mediators Inflamm 2013;2013:752519.

54. Chaly Y, Hostager B, Smith S, Hirsch R. Follistatin-like protein 1 and its role in inflammation and inflammatory diseases. Immunol Res 2014;59:266–72.

55. van Empel V, Brunner-La Rocca HP. Inflammation in HFpEF: key or circumstantial? Int J Cardiol 2015;189:259–63.

56. Kaess BM, Vasan RS. Heart failure: pentraxin 3—a marker of diastolic dysfunction and HF? Nat Rev Cardiol 2011;8:246–8.

KEY WORDS **cardiac hypertrophy, follistatin-like 1, heart failure with preserved ejection fraction**